ANTICANCER RESEARCH *32*: xxx-xxx (2012)

No: 14571-R
Please mark the appropriate section for this paper
☐ Experimental
☐ Clinical
☐ Epidemiological

MRI and Ultrasound-guided Prostate Biopsy Using Soft Image Fusion

ERIK RUD[1], EDUARD BACO[2] and HEIDI B. EGGESBØ[1,3]

[1]*Division of Diagnostics and Intervention, Department of Radiology and Nuclear Medicine, Oslo University Hospital, Aker, Norway;*
[2]*Division of Surgery and Cancer Medicine, Department of Urology, Oslo University Hospital, Aker, Norway;*
[3]*Division of Diagnostics and Intervention, Department of Radiology and Nuclear Medicine, Oslo University Hospital, Rikshospitalet, Norway*

Abstract. *Objectives: Transrectal ultrasound (TRUS) guided random biopsies is the gold standard when diagnosing prostate cancer. A new 3D system with organ tracking, allows accurate targeted biopsies using magnetic resonance imaging (MRI) and TRUS soft image fusion. The aim of the study was to evaluate the accuracy of targeted biopsies. Materials and Methods: Retrospective study of 90 consecutive patients with suspected prostate cancer underwent MRI prior to biopsy using 3D T2w and diffusion weighted imaging (12 min protocol). Suspicious tumours (MRI targets) were highlighted on axial T2w images and classified as high, moderate or low degree of cancer suspicion. Navigation system: Urostation(Koelis®, Grenoble, France). Primary endpoint: Rate of successful targeted biopsies. Positive biopsies with Gleason score. Results: MRI was positive in 80/90 (89%) patients, in which 115 MRI targets were identified and biopsied. There were 112/115 (97%) successful biopsies inside target, and 60/115 (52%) targets were positive for cancer. Positive biopsies according to degree of cancer suspicion were: high 50/55 (91%), medium 6/22 (27%) and low 4/38 (10%). All MRI negative patients had negative random biopsies. Conclusion: The high rate (97%) of successful biopsies in this study indicates that targeted biopsies using MRI and TRUS soft image fusion technique might be an accurate method.*

The use of magnetic resonance imaging (MRI) prior to prostate biopsy is commonly used for tumour detection (1-3). However, conventional biopsies cannot verify that it is actually the cancer suspicious MRI targets that have been biopsied. It might cause a diagnostic dilemma in case of a positive MRI finding, and negative biopsy. This is why different image fusion systems, with different ranges of targeting error have been developed in order to provide MRI targeted biopsies (4-11).

A new soft image fusion system with organ tracking provides 3D image documentation of the biopsy track. The method allows both virtual and targeted biopsies of suspicious areas identified on MRI. The 3D biopsy map shows the spatial distribution of the biopsies performed, and verifies that all regions are sampled. In addition, the distribution of positive and negative biopsies can be used for planning treatment or supplementary biopsies, if needed. The targeting error of the system used in this study is estimated to be 0.76±0.52 mm (12).

The aim of this study was to evaluate the accuracy of targeted biopsies using MRI and TRUS soft image fusion technique.

Materials and Methods

Ninety patients referred to prostate biopsy due to elevated prostate specific antigen (PSA) were included between December 2010 and May 2011. The study was performed as a quality control study with permission from the local Ethical Committee at Oslo University Hospital. Eleven patients were referred for the initial (first) biopsy, 62 for re-biopsy (first-sixth), and 17, due biochemical recurrence (BCR) after radiotherapy (RT). The clinical data is summarized in Table I. All previous biopsies had been performed using standard TRUS method by urologists at university hospitals or private outpatient clinics. The PSA registered was the latest value measured prior to the biopsy. The prostate volume was measured using TRUS during the biopsy procedure.

MRI procedure. All MRI examinations were performed immediately prior to the biopsy session on a 1. 5 Tesla Avanto® MRI (Siemens, Erlangen, Germany) using a 6-channel Body MATRIX® coil

Correspondence to: Erik Rud, Division of Diagnostics and Intervention, Department of Radiology and Nuclear Medicine, Oslo University Hospital, Aker, Trondheimsveien 235, 0514 Oslo, Norway. Tel: +47 9344564 (mobile), +47 22894411 (direct), Fax: +47 23033046, e-mail: p.e.rud@medisin.uio.no

Key Words: Prostate cancer, soft-image fusion, MRI, TRUS, targeted biopsy.

Table I. *Demographic and clinical data of 90 patients referred for biopsy due to elevated prostate specific antigen (PSA) and suspected prostate cancer.*

Biopsy group	n	Median age (years) (range)	Median PSA (ng/ml) (range)	Median volume (ml) (range)
Initial biopsy	11	64 (52-77)	7.3 (5-74)	30 (9-42)
First re-biopsy	24	62 (50-75)	5.8 (2-14)	29 (13-70)
Second re-biopsy	18	63 (55-73)	9.9 (5-46)	36 (24-115)
Third re-biopsy	8	64 (61-80)	19.1 (9-39)	29 (20-47)
Fourth re-biopsy	4	64 (63-66)	16.2 (6-27)	74 (35-100)
Fifth re-biopsy	7	66 (54-70)	14.4 (12-31)	50 (23-95)
Sixth re-biopsy	1	77 (77)	50.0 (55)	58 (58)
Biopsy after RT	17	69 (51-79)	4.5 (1-18)	19 (8-40)
Total no. of patients	90	64 (50-80)	7.0 (1-74)	28 (8-115)

RT: Radiotherapy.

Table II. *MRI sequences and acquisition parameters.*

Sequence	Slice thickness (mm)	FOV (mm)	Matrix (pixels)	TR (ms)	TE (ms)	BW	b Value	Scan time (min:sec)
Sag T2tse	5	380×272	162×256	2900	97	201		00:45
Ax T2spc*	1	292×292	384×387	2000	123	650		07:02
Ax DWI	4	300×300	128×128	2600	81	1648	50, 1000	03:15
AxDWI	5	250×250	68×114	2400	120	1512	2000	01:34

FOV: Field of view, TR: time of repetion, TE: time of echo, BW: band width. *T2spc: High resolution 3D aquisition with 0.9mm isotropic voxels.

(Siemens, Erlangen, Germany). All patients were asked to empty their bladder and bowel prior to examination. No anti-peristaltic drugs were administered. The sequences used were: axial 3D T2 weighted (T2w), axial diffusion weighted imaging (DWI) with apparent diffusion (ADC) map calculated from b50 and b1000. In addition an axial DWI using b2000 was obtained. The MRI acquisition parameters are summarized in Table II.

MRI post processing procedures. The software program nordic ICE® (NordicNeuroLab, Bergen, Norway) was used for colour highlighting different DWI parameters, and a drag and drop overlay technique was used to superimpose semi-transparent colour maps onto the T2w images (Figure 1). Colour maps with the following DWI parameters were used: i) T2-corrected b1000, ii) ADC and iii) b2000. T2-corrected b1000 images were used in order to avoid the T2 shine through as seen in native DWI. Cut-off values used to remove noise and highlight areas of interest were: ADC map (mm^2/s): min 50×10^{-5} and max 250×10^{-5}, T2-corrected b1000 signal intensity (SI): min 30, max 35, b2000 (SI): min 10, max 15.

Definition of cancer suspicious regions (MRI targets). Tumour suspicion was defined according to the following parameters:
Signal quality: Tumour signal was defined as homogenous intermediate low T2 signal (between fat and muscle).
Signal intensity (T2-corrected b1000, ADC and b2000): High signal areas relative to muscle in T2-corrected b1000 images and b2000.

Table III. *MRI and biopsy results in 90 patients with suspected prostate cancer.*

	Biopsy results, n (%)				Total	
MRI	Positive		Negative			
Positive	54	68	26	32	80	89
Negative	0	0	10	100	10	11

ADC value $<130\times10^{-5}$ mm^2/s in peripheral zone and $<100\times10^{-5}$ mm^2/s in the transition zone.
Location of the tumour: Tumours in the peripheral zone and ventral part of the transition zone (ventral to urethra) were regarded as more suspicious than similar findings in the posterior part of the transition zone since these areas are known to harbour the vast majority of tumours (13-16).
Tumour size: The largest diameter served as the reference for tumour size (17).
Tumour shape: Lenticular shaped and poorly defined areas were defined as suspicious (13, 18, 19).

Classification on MRI findings. Presence or absence of MRI targets: Each MRI examination was classified as either positive or negative with respect to presence of MRI targets.

Table IV. *Biopsy results of 115 MRI targets in 80 patients with respect to the degree of cancer suspicion at MRI.*

Degree of MRI tumour suspicion	Number of MRI targets	Biopsy verified inside the MRI target, n(%)		Biopsy results, n(%)		Others*, n	
		Yes	No	Positive	Negative	ASAP	Inflammation
High	55	54 (98)	1 (2)	50 (91)	5 (9)	1	0
Medium	22	21 (95)	1 (5)	6 (27)	16 (73)	0	1
Low	38	37 (97)	1 (3)	4 (10)	34 (90)	3	1
Total	115 (100)	112 (97)	3 (3)	60 (52)	55 (49)	4	2

Biopsies outside target (three patients) were classified as negative. *Defined as negative biopsies, including atypical small acinar cell proliferation (ASAP) and inflammation.

Classification of MRI targets according to degree of cancer suspicion: Each MRI target was sub classified as having a low, moderate, or high degree of cancer suspicion depending on how many sequences the tumour was visible: high degree (all sequences), moderate degree (two or three sequences) and low degree (one or two sequences). This is similar to a system used by Pinto *et al*. (7).

A maximum of three cancer suspicious areas were identified in each patient and termed MRI target 1, 2 and 3 according to the size, where MRI target 1 was the largest.

MRI and ultrasound soft image fusion procedure: The technical details of the soft image fusion acquisition have been described in a previous study (12). Key features of this system are organ tracking and compensation for tissue deformation during the procedure. Organ tracking means that the prostate gland is the geometrical reference during the procedure, making it unsusceptible to patient movement. Compensation of gland deformation during the procedure is essential in order to obtain the highest possible accuracy and reduce the range of targeting error.

Three essential steps are involved in the fusion process:

Firstly: Prior to the biopsies, the MRI T2w sequence was loaded into the Urostation® (Koelis, Grenoble, France). In a semiautomatic process, the system registered the prostate volume in 3D, and suspicious areas were manually highlighted as red spherical targets on the axial T2w images. The targets were made small enough to ascertain that a successful biopsy truly was inside the suspected tumour and they were directed towards the areas with the lowest ADC signal. The diameters of the targets were 4-6 mm (volume 0.03-0.1 ml).

Secondly: A TRUS examination obtained a 3D volume of the prostate gland using an ultrasound probe with an internally rotating head. The final step involved software fusion of the MRI and ultrasound volumes. This is in accordance to the process described by Cornud *et al*. (20).

Biopsy procedure: All biopsies were performed using a real-time transrectal ultrasound end-fire probe (3D AccuvixV10; Medison® Korea) with 18Gx25cm biopsy needle (True-Core®II; Angiotech, Vancouver, Canada).

Each biopsy was immediately followed by a 3D-TRUS acquisition (3-5 s) with the needle still in the prostate gland. Both the needle track and the MRI target were displayed on the fused volume. The accuracy of biopsy needle position has been evaluated as being 0.76±0.52 mm (12, 20).

Targeted biopsies: A minimum of two biopsies was obtained from each MRI target. After each biopsy the needle was visualized in 3D within the gland in order to evaluate whether the biopsy had been within the MRI target or not.

Random biopsies: 12-Core biopsy procedures were performed in all MRI-negative and selected MRI-positive patients. Selection criteria for the MRI-positive patients was based on age, PSA, degree of MRI findings, number of previous biopsies and whether focal treatment was an option or not. Both targeted and random biopsy needle tracks were saved in 3D for retrospective evaluation. A superimposed sextant grid was used to improve the spatial distribution of random biopsies (Figure 2b).

Histopathological procedure: The biopsies were examined by uropathologists and classified as either positive or negative. Positive biopsies were scored according to the Gleason scoring system (21). Gleason score 7A and 7B were combined as Gleason score 7.

Unsuccessful biopsies, atypical small acinar cell proliferation (ASAP) and inflammation were classified as negative biopsies.

Evaluation of the biopsy location: The needle track was visualized in real-time during the procedure and documented and stored in 3D fusion images using the software provided. As a rule, random biopsies were obtained from MRI-negative areas (*i.e*. no cancer-suspicious areas).

Results

Positive MRI examination was found in 80/90 (89%) and 54/90 (60%) had a positive biopsy. All ten patients with negative MRI had negative biopsies. The overall accuracy of MRI was 64/90 (71%) using the biopsy results as the reference.

In 80 patients 115 MRI targets were identified. Successful biopsies (*i.e*. biopsy inside the MRI target) were achieved in 112/115 (97%), of which 60/115 (52%) were positive for cancer. The degrees of cancer suspicion for the 115 MRI targets were high in 55/115 (48%), medium in 22/115 (19%), and low in 38/115 (33%).

Positive biopsies with respect to the degree of cancer suspicion on MRI were high: 50/55 (91%), medium: 6/22 (27%) and low: 4/38 (10%). The results of MRI findings and targeted biopsies are summarized in Table III and IV.

Forty-two patients underwent random biopsies: all of the patients with a negative MRI and 32 patients with a positive MRI. Positive biopsies were found in 6/42 (14%), all in patients with positive targeted biopsies. Four patients had

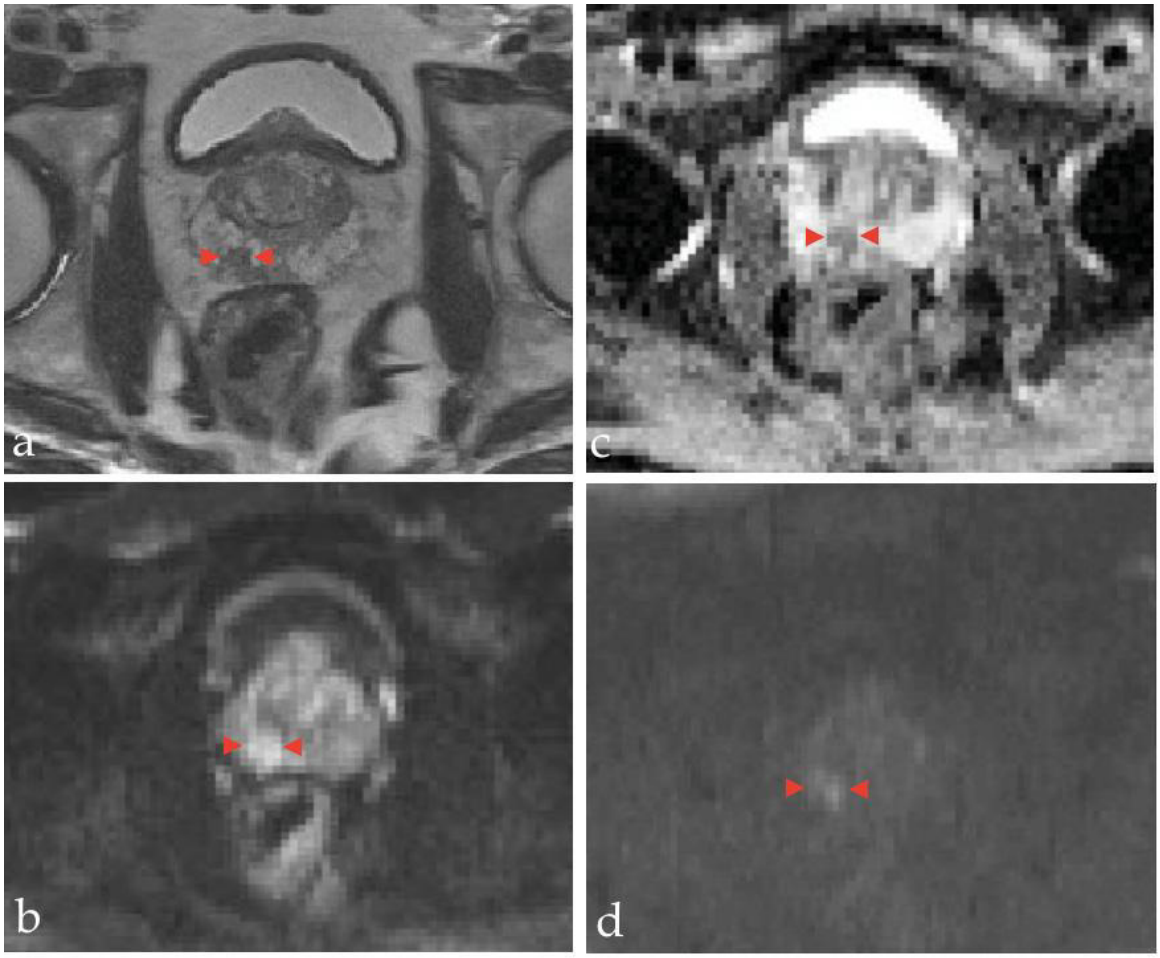

Figure 1 Continued

Gleason score 6, and two had Gleason score 7. Retrospective evaluation of the MR images could identify 4/6 cancers, while two could not be identified. One of these foci were Gleason score 7. However, none of the positive random biopsies caused an overall upgrading of the Gleason score in any patient, as all patients had identical Gleason score in the targeted biopsy. All patients with negative MRI had negative random biopsies. The Gleason scores according to the biopsy groups are summarized in Table V.

Discussion

The main limitation of this study is the selection of patients. Our hospital is a referral hospital for a larger region, and we included a very heterogeneous and selected patient group. This makes it impossible to compare the results to those of other studies.

However, the main question when evaluating the accuracy of this method is whether the needle was within the MRI target or not. In previous studies, the range of targeting error using the Urostation® is reported to be around 1 mm (4, 12).

Three important factors imply a high clinical accuracy: Firstly; real-time 3D TRUS enables biopsy visualization and documentation, both during the procedure and retrospectively. Secondly, the high rate of positive biopsies in MRI targets with a high degree of cancer suspicion indicates that the needle was in the desired location. Thirdly, the target volumes were not larger than 0.1 ml, which might indicate that targeted biopsies from small lesions are indeed possible.

Criteria for selecting patients for random biopsies were not rigid. When MRI identified a highly suspicious tumour in a patient with several previous negative biopsies, only targeted biopsies were performed. However, patients without previous biopsies, or unilateral findings, underwent both targeted and random biopsies in order to select patients for focal therapy as proposed by Baco *et al.* at the 4th International Symposium on Focal Therapy and Imaging in Prostate and Kidney Cancer 2011, Leiden, Holland.

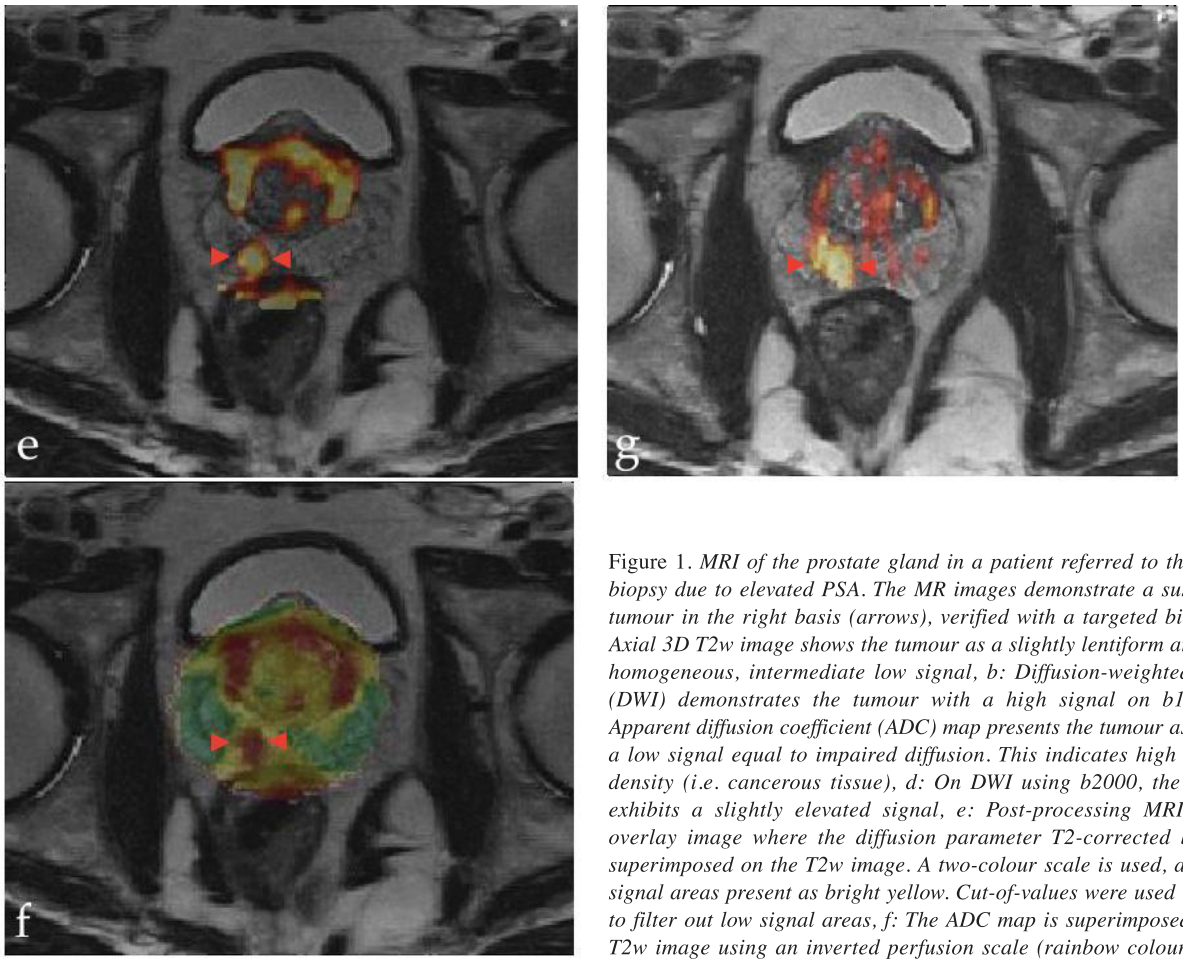

Figure 1. *MRI of the prostate gland in a patient referred to the initial biopsy due to elevated PSA. The MR images demonstrate a suspicious tumour in the right basis (arrows), verified with a targeted biopsy. a: Axial 3D T2w image shows the tumour as a slightly lentiform area with homogeneous, intermediate low signal, b: Diffusion-weighted image (DWI) demonstrates the tumour with a high signal on b1000, c: Apparent diffusion coefficient (ADC) map presents the tumour as having a low signal equal to impaired diffusion. This indicates high cellular density (i.e. cancerous tissue), d: On DWI using b2000, the tumour exhibits a slightly elevated signal, e: Post-processing MRI colour overlay image where the diffusion parameter T2-corrected bmax is superimposed on the T2w image. A two-colour scale is used, and high signal areas present as bright yellow. Cut-of-values were used in order to filter out low signal areas, f: The ADC map is superimposed on the T2w image using an inverted perfusion scale (rainbow colour scale). Cut-off values were adjusted in order for the red-pink-white colours represent low ADC values (<100 mm^2/s), while green/blue reveals high ADC values (>170 mm^2/s), g: This image demonstrates the superimposed b2000 image. A two-colour scale is used as described in (e). It displays the improvement of the spatial resolution, and the ability to detect tumours well when compared to the native b2000.*

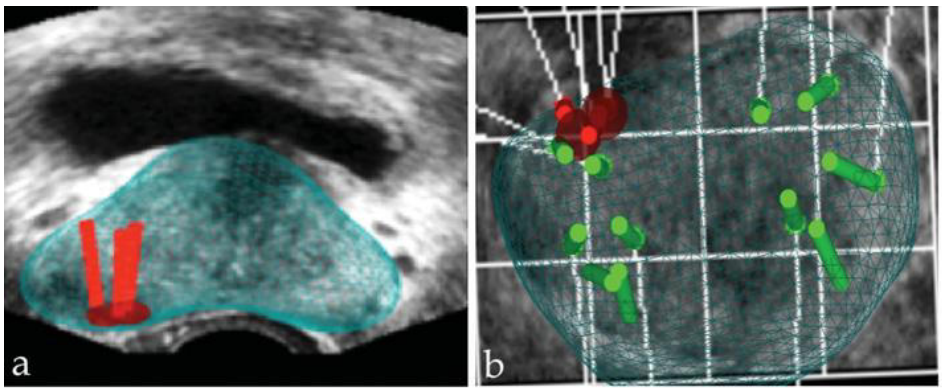

Figure 2. *a: Axial real-time fusion image as seen by the operator when performing the targeted biopsies. The image shows the suspicious tumour marked as a red circle within the prostate volume. The biopsies were documented inside the MRI target and appear as red cylinders. Histopathological results showed Gleason score 3+4 in this case. b: Coronal real time fusion image shows the spatial distribution of random biopsies in a MRI-positive patient. The histopathological results of random biopsies were negative, and marked as green. The superimposed grid helps obtain biopsies from all sextants.*

Table V. *Biopsy results with respect to Gleason score in 90 patients.*

Biopsy group	Patients, n	Biopsy results, n(%)				Other*, n	Gleason Score			
		Positive		Negative			6	7	8	9
Initial biopsy	11	9	82	2	18	1	3	3	2	1
First re- biopsy	23	13	58	10	42	1	6	5	2	0
Second re- biopsy	18	9	50	9	50	0	4	2	3	0
Third re- biopsy	8	6	75	2	25	1	1	3	2	0
Fourth re- biopsy	4	0	0	4	100	0	0	0	0	0
Fifth re- biopsy	7	2	29	5	71	1	1	1	0	0
Sixth re- biopsy	1	1	100	0	0	0	0	1	0	0
Biopsy after RT	18	14	82	4	18	0	2	7	4	1
Total	90	54	61	36	39	4	17	22	13	2

*Defined as negative biopsies including ASAP and inflammation. RT: Radiotherapy. Gleason score 7A and 7B were both classified as Gleason score 7.

Tan *et al*. (22) showed that only the detection rate of small and insignificant cancer increased in case of re-biopsies. However, we found 28/59 (47%) positive biopsies in the patient group undergoing the first, second and third re-biopsy, and 17/28 (60%) were of Gleason score 7 and 8.

Since only a few patients have undergone prostatectomy, we were unable to perform reliable statistical tests in order to present sensitivity and specificity. Therefore, the true rate of false-positive and -negative findings remains unknown.

MRI protocol and detection of tumours. Lately, consensus reports and guidelines have been published in order to recommend a MRI protocol, and define tumour-suspicious areas (13). Our protocol differed in some aspects. Most importantly, we did not use dynamic contrast enhancement (DCE), and we did not use an endorectal coil. This might reduce the sensitivity of MRI. However, few publications have actually compared the performance of DCE and DWI using prostatectomy as the reference. One study (n=58) found that DCE performed slightly better in the peripheral zone when combined with DWI than DWI performed alone (AUC=0.90, 95% CI=0.86-0.93 *vs*. AUC=0.84, 95% CI=0.80-0.88). No differences were found in the transitional zone (14). Recently, a biopsy study (n= 168) compared the performance of DCE and DWI, and found a better performance of DWI compared to DCE, although not significantly (23).

The definition and classification of the degree of tumour suspicion is subject to controversy, although a recent attempt has been made in order to standardize the criteria (13). An important reason why we did not use the PI-RADS criteria described in the ESUR 2012 guidelines is because we did not use DCE-MRI. The criteria for tumour detection using the other sequences were similar, although the actual scoring system was different. In this study, we defined the degree of suspicion based upon how many sequences the suspected tumour was visible. As noted previously, this is similar to classification system used by Pinto *et al*., although not based on the same sequences (7). This classification method is highly susceptible to interobserver variability, which is another major limitation in this study.

Future Aspects

A more accurate biopsy technique might reduce the need for both random biopsies and re-biopsies. Furthermore, targeted biopsies should be implemented in the diagnostic workup before deciding type of curative treatment or active surveillance (4).

Conclusion

The high rate (97%) of successful biopsies in this study indicates that targeted biopsies using MRI and TRUS with a soft image fusion technique might be an accurate method.

Acknowledgements

The foundation *AKTIV* against cancer® funded the purchase of ultrasound equipment and software used in this study.

References

1 Hambrock, T, Somford, DM, Hoeks C, Bouwense SAW, Huisman H, Yakar D, van Oort IM, Witjes JA, Fütterer JJ and Barentsz JO: Magnetic Resonance Imaging Guided Prostate Biopsy in Men With Repeat Negative Biopsies and Increased Prostate Specific Antigen. JURO *183*: 520-528, 2010.

2 Cheikh AB, Girouin N, Colombel M, Maréchal JM, Gelet A, Bissery A, Rabilloud M, Lyonnet D and Rouvière O: Evaluation of T2-weighted and dynamic contrast-enhanced MRI in localizing prostate cancer before repeat biopsy. Eur Radiol *19*: 770-778, 2008.

3 Park BK, Lee HM, Kim CK, Choi HY and Park JW: Lesion Localization in Patients With a Previous Negative Transrectal Ultrasound Biopsy and Persistently Elevated Prostate Specific

Antigen Level Using Diffusion-Weighted Imaging at Three Tesla Before Rebiopsy. Invest Radiol *43*: 789-793, 2008.
4 Ukimura O: Evolution of precise and multimodal MRI and TRUS in detection and management of early prostate cancer. Expert Rev Med Dev *7*: 541-554, 2010.
5 Ukimura O, Faber K and Gill IS: Intraprostatic targeting. Curr Opini Urol *22*: 97-103, 2012.
6 Hadaschik, BA, Kuru TH, Tulea C, Rieker P, Popeneciu IV, Simpfendörfer T, Huber J, Zogal P, Teber D, Pahernik S, Roethke M, Zamecnik P, Roth W, Sakas G, Schlemmer HP and Hohenfellner M: A novel stereotactic prostate biopsy system integrating pre-interventional magnetic resonance imaging and live ultrasound fusion. J Urol *186*: 2214-2220, 2011.
7 Pinto PA, Chung PH, Rastinehad AR, Baccala AA Jr., Kruecker J, Benjamin CJ, Xu S, Yan P, Kadoury S, Chua C, Locklin JK, Turkbey B, Shih JH, Gates SP, Buckner, C, Bratslavsky G, Linehan WM, Glossop ND, Choyke PL and Wood BJ: Magnetic Resonance Imaging/Ultrasound Fusion Guided Prostate Biopsy Improves Cancer Detection Following Transrectal Ultrasound Biopsy and Correlates With Multiparametric Magnetic Resonance Imaging. JURO *186*: 1281-1285, 2011.
8 Turkbey B, Xu S, Kruecker J, Locklin J, Pang Y, Bernardo M, Merino MJ, Wood B. J, Choyke PL and Pinto PA: Documenting the location of prostate biopsies with image fusion. BJU Int *107*: 53-57, 2010.
9 Hu Y, Ahmed H, Taylor Z and Allen C: MR to ultrasound registration for image-guided prostate interventions. Med Image Anal *16*: 687-703, 2012.
10 Xu S, Kruecker J, Turkbey B, Glossop N, Singh AK, Choyke P, Pinto P and Wood BJ: Real-time MRI-TRUS fusion for guidance of targeted prostate biopsies. Comput Aided Surg *13*: 255-264, 2008.
11 Yan P, Xu S, Turkbey B and Kruecker J: Discrete deformable model guided by partial active shape model for TRUS image segmentation. IEEE Trans Biomed Eng *57*: 1158-1166, 2010.
12 Baumann M, Mozer P, Daanen V and Troccaz J: Prostate biopsy tracking with deformation estimation. Med Image Anal *16*: 562-576, 2011.
13 Barentsz JO, Richenberg J, Clements R, Choyke P, Verma S, Villeirs G, Rouvière, O, Logager V and Futterer JJ: ESUR prostate MR guidelines 2012. Eur Radiol 2012.
14 Delongchamps NB, Beuvon F, Eiss D, Flam T, Muradyan N, Zerbib M, Peyromaure M and Cornud F: Multiparametric MRI is helpful to predict tumor focality, stage, and size in patients diagnosed with unilateral low-risk prostate cancer. Prostate Cancer Prostatic Dis *14*: 232-237, 2011.
15 Coakley FV and Hricak H: Radiologic anatomy of the prostate gland: a clinical approach. Radiol Clin North Am *38*: 15-30, 2000.
16 Verma S and Rajesh A: A Clinically Relevant Approach to Imaging Prostate Cancer: Review. Am J Roentgenol *196*: S1-S10, 2011.
17 van der Kwast TH, Amin MB, Billis A, Epstein JI, Griffiths D, Humphrey PA, Montironi R, Wheeler TM, Srigley JR, Egevad L, Delahunt B and Group, T. I. P. C: International Society of Urological Pathology (ISUP) Consensus Conference on Handling and Staging of Radical Prostatectomy Specimens. Working group 2: T2 substaging and prostate cancer volume. Mod Pathol *24*: 16-25, 2010.
18 Girouin N, Mège-Lechevallier F, Tonina Senes A, Bissery A, Rabilloud M, Maréchal JM, Colombel M, Lyonnet D and Rouvière O: Prostate dynamic contrast-enhanced MRI with simple visual diagnostic criteria: is it reasonable? Eur Radiol *17*: 1498-1509, 2006.
19 Lemaitre L, Puech P, Poncelet E, Bouyé S, Leroy X, Biserte J and Villers A Dynamic contrast-enhanced MRI of anterior prostate cancer: morphometric assessment and correlation with radical prostatectomy findings. Eur Radiol *19*: 470-480, 2008.
20 Cornud F, Delongchamps NB, Mozer P, Beuvon F, Schull A, Muradyan N and Peyromaure, M. Value of Multiparametric MRI in the Work-up of Prostate Cancer. Curr Urol Rep *13*: 82-92, 2011.
21 Epstein JI: An Update of the Gleason Grading System. JURO *183*: 433-440, 2010.
22 Tan N, Lane BR, Li J, Moussa AS, Soriano M and Jones JS: Prostate Cancers Diagnosed at Repeat Biopsy are Smaller and Less Likely to be High Grade. J Urol *180*: 1325-1329, 2008.
23 Iwazawa J, Mitani T, Sassa S and Ohue S: Prostate cancer detection with MRI: is dynamic contrast-enhanced imaging necessary in addition to diffusion-weighted imaging? Diagn Interv Radiol *17*: 243-248, 2011.

Received March 15, 2012
Revised April 23, 2012
Accepted April 24, 2012